Journal of Physics: Conference Series **597** (2015) 012054 doi:10.1088/1742-6596/597/1/012054

Emergent symmetries in atomic nuclei from first principles

K D Launey, A C Dreyfuss, R B Baker, J P Draayer and T Dytrych

Department of Physics and Astronomy, Louisiana State University,
Baton Rouge, LA 70803, USA

E-mail: kristina@baton.phys.lsu.edu

Abstract. An innovative symmetry-guided approach and its applications to light and intermediate-mass nuclei is discussed. This approach, with Sp(3,$\mathbb{R}$) the underpinning group, is based on our recent remarkable finding, namely, we have identified the symplectic Sp(3,R) as an approximate symmetry for low-energy nuclear dynamics. This study presents the results of two complementary studies, one that utilizes realistic nucleon-nucleon interactions and unveils symmetries inherent to nuclear dynamics from first principles (or *ab initio*), and another study, which selects important components of the nuclear interaction to explain the primary physics responsible for emergent phenomena, such as enhanced collectivity and alpha clusters. In particular, within this symmetry-guided framework, *ab initio* applications of the theory to light nuclei reveal the emergence of a simple orderly pattern from first principles. This provides a strategy for determining the nature of bound states of nuclei in terms of a relatively small fraction of the complete shell-model space, which, in turn, can be used to explore ultra-large model spaces for a description of alpha-cluster and highly deformed structures together with associated rotations. We find that by using only a fraction of the model space extended far beyond current no-core shell-model limits and a long-range interaction that respects the symmetries in play, the outcome reproduces characteristic features of the low-lying 0^+ states in ^{12}C (including the elusive Hoyle state of importance to astrophysics) and agrees with *ab initio* results in smaller spaces. For these states, we offer a novel perspective emerging out of no-core shell-model considerations, including a discussion of associated nuclear deformation, matter radii, and density distribution. The framework we find is also extensible beyond ^{12}C, namely, to the low-lying 0^+ states of ^{8}Be as well as the ground-state rotational band of Ne, Mg, and Si isotopes.

1. Introduction

Approximate symmetries in atomic nuclei that favor large deformation along with monopole and quadrupole excitations thereof, associated with the SU(3) group and the symplectic Sp(3,$\mathbb{R}$) group, have been long recognized in selected cases [1–10]. But only recently, we have confirmed the existence of these symmetries, within the *ab initio* (or "from first principles") symmetry-adapted no-core shell model (SA-NCSM) framework [11]. This study unveiled the orderly patterns associated with such symmetries in nuclear wavefunctions from first principles, without *a priori* symmetry constraints. This suggests a novel theoretical framework for nuclear structure modeling that, in addition to the exact conventional symmetries, such as parity and rotational invariance, can take advantage of these approximate symmetries. The latter are utilized and further understood in the framework of the microscopic no-core symplectic model (NCSpM) [12],

which combines a long-range many-nucleon interaction that respects the symmetries in play together with a symmetry-mixing spin-orbit term. The findings of the present study point to a new insight, namely, understanding the mechanism and the primary physics responsible for the emergence of simple structures in complex nuclei from a no-core shell-model perspective.

One of the most successful particle-driven models is the *ab initio* no-core shell model (NCSM) [13], which can accommodate any type of inter-nucleon interactions, including modern two- and three-nucleon realistic interactions. Specifically, for a general problem, the NCSM adopts the intrinsic non-relativistic nuclear plus Coulomb interaction Hamiltonian defined as follows:

$$H = T_{\rm rel} + V_{NN} + V_{NNN} + \ldots + V_{\rm Coulomb}, \tag{1}$$

where the V_{NN} nucleon-nucleon interaction is included along with the $V_{\rm Coulomb}$ Coulomb interaction between the protons. The Hamiltonian may include a V_{NNN} 3-nucleon interaction and additional terms such as multi-nucleon interactions among more than three nucleons simultaneously and higher-order electromagnetic interactions such as magnetic dipole-dipole terms. It adopts the harmonic oscillator (HO) single-particle basis characterized by the $\hbar\Omega$ oscillator strength (or equivalently, the oscillator length $b = \sqrt{\frac{\hbar}{m\Omega}}$ for a nucleon mass m) and retains many-body basis states of a fixed parity, consistent with the Pauli principle, and limited by a cutoff $N_{\rm max}$. The $N_{\rm max}$ cutoff is defined as the maximum number of HO quanta allowed in a many-body basis state above the minimum for a given nucleus. It divides the space in "horizontal" HO shells and is dictated by particle-hole excitations (this is complementary to the NCSpM, which divides the space in vertical slices selected by collectivity-driven rules). It seeks to obtain the lowest few eigenvalues and eigenfunctions of the Hamiltonian (1). The NCSM has achieved remarkable descriptions of low-lying states from the lightest nuclei up through ^{12}C, ^{16}O, and ^{14}F [13, 14], and is further augmented by several techniques, such as NCSM/RGM [15], Importance Truncation NCSM [16] and Monte Carlo NCSM [17]. This supports and complements results of other first-principle approaches, such as Green's function Monte Carlo (GFMC) [18], Coupled-cluster (CC) method [19], In-Medium SRG [20], and Lattice Effective Field Theory (EFT) [21].

However, the established NCSM methods are not able to reach the physics regime necessary for a description of largely deformed nuclear states, such as the ^{12}C Hoyle state that was predicted based on observed abundances of heavy elements in the universe [22], and which has attracted much recent attention both in theory (e.g., see [21, 23, 24]) and experiment ([25–32]). In this study, we address this problem, within a no-core shell-model framework, by utilizing a small subset of symplectic $\mathrm{Sp}(3,\mathbb{R})$ basis states [6, 7] (with the complete set yielding results equivalent to those of the NCSM), an $\mathrm{Sp}(3,\mathbb{R})$-preserving part of the long-range inter-nucleon interaction [12], and an important symmetry-breaking spin-orbit term.

2. Discovery of a highly structured pattern within the first-principle SA-NCSM framework

The *ab initio* symmetry-adapted no-core shell model (SA-NCSM) [11] combines the first-principle concept of the NCSM with symmetry-guided considerations. For the first time, we show the emergence – in the framework of the SA-NCSM from first principles – of orderly patterns that favor large deformation/low spin in nuclear wavefunctions [11]. These patterns are linked to the SU(3) group and the symplectic $\mathrm{Sp}(3,\mathbb{R})$ group, where $\mathrm{Sp}(3,\mathbb{R})\supset\mathrm{SU}(3)$. SU(3) describes the 3-dimensional harmonic oscillator and its irreducible representations (irreps) are specified by $(\lambda_\omega\,\mu_\omega)$ quantum numbers that can be related to the intrinsic quadrupole deformation [33–35] – e.g., $(0\,0)$, $(\lambda_\omega\,0)$, and $(0\,\mu_\omega)$ describe spherical, prolate, and oblate shapes, respectively. The $\mathrm{Sp}(3,\mathbb{R})$ group is described in detail in Section 3.

In particular, the *ab initio* $N_{\rm max} = 8$ SA-NCSM results with the bare N^{3}LO [36] (similarly, for JISP16 [37]) realistic interaction for the ^{8}Be 0^+ ground state (*gs*) and its rotational band

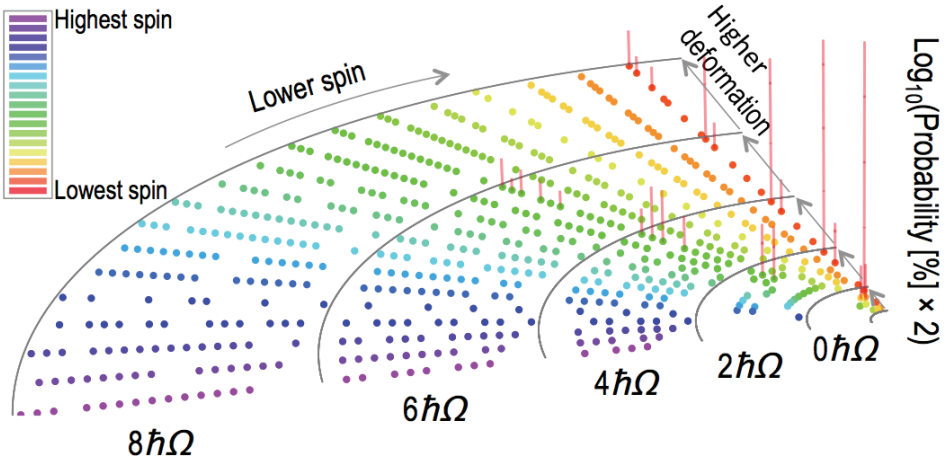

Figure 1. Probability distribution across Pauli-allowed intrinsic spin and deformation configurations for the *ab initio* SA-NCSM 0^+ *gs* of ^{8}Be for $N_{\max} = 8$ and $\hbar\Omega = 25$ MeV with the N^{3}LO interaction. The concentration of strengths to the far right demonstrates the dominance of collectivity in the calculated eigenstates. This novel feature enables the SA-NCSM – by using symmetry-dictated subspaces – to reach new domains currently inaccessible by *ab initio* calculations, such as isotopes of Ne, Mg, and Si.

reveal the dominance of the $0\hbar\Omega$ component with the foremost contribution coming from the leading $(\lambda_\omega\,\mu_\omega) = (4\,0)$ SU(3) irrep (Fig. 1). Furthermore, we find that important SU(3) configurations are then organized into structures according to the Sp$(3,\mathbb{R})$ symplectic group, that is, the $(\lambda_\sigma\,\mu_\sigma) = (4\,0)$ $S = 0$ symplectic irrep contains the $(\lambda_\omega\,\mu_\omega) = (4\,0)$ configuration in the $0\hbar\Omega$ subspace, $(\lambda_\omega\,\mu_\omega) = (6\,0)$, $(4\,1)$, and $(2\,2)$ configurations in the $2\hbar\Omega$ subspace, and so on. Those configurations, all part of a single symplectic irrep, the $S = 0$ $(4\,0)$, indeed realize the major components of the wavefunction in the respective subspaces. Similar results are observed for other *p*-shell nuclei, such as ^{6}Li, ^{6}He, and ^{12}C. This further reveals the significance of the symplectic symmetry to nuclear dynamics. Moreover, the outcome supports a symmetry-guided concept [11], based on the dominance of only a few configurations, as evident by the concentration of probability to the far right in Fig. 1. That the relevant model space can be systematically selected, using a quantified cutoff, starting from the largest deformation and associated symplectic excitations thereof, and including ever smaller deformation until convergence of results is achieved, is a key feature of the SA-NCSM.

3. Symplectic Sp$(3,\mathbb{R})$ group

The significance of the symplectic Sp$(3,\mathbb{R})$ group for a microscopic description of a quantum many-body system of interacting particles has been recognized by Rowe and Rosensteel [6, 7]. Indeed, the 21 symplectic generators are directly related to the particle momentum $(p_{s\alpha})$ and coordinate $(r_{s\alpha})$ operators, with $\alpha = x$, y, and z for the 3 spatial directions and s labeling an individual nucleon, and realize important observables. Namely, Sp$(3,\mathbb{R})$-preserving operators include: the many-particle kinetic energy $\sum_{s,\alpha} p_{s\alpha}^2/2m$, the HO potential, $\sum_{s,\alpha} m\Omega^2 r_{s\alpha}^2/2$, the mass quadrupole moment $Q_{(2\mathcal{M})} = \sum_s q_{(2\mathcal{M})s} = \sum_s \sqrt{16\pi/5}\, r_s^2 Y_{(2\mathcal{M})}(\hat{\mathbf{r}}_s)$, and angular momentum L operators, together with multi-shell collective vibrations and vorticity degrees of freedom for a description from irrotational to rigid rotor flows. Indeed, an important Sp$(3,\mathbb{R})$-preserving interaction is $\frac{1}{2}Q\cdot Q = \frac{1}{2}\sum_s q_s \cdot (\sum_t q_t)$, as this realizes the physically relevant interaction of each particle with the total quadrupole moment of the nuclear system.

The symplectic $\mathrm{Sp}(3,\mathbb{R})$ symmetry underpins the symplectic shell model, which provides a microscopic formulation of the Bohr-Mottelson collective model [1] and is a multiple oscillator shell generalization of the successful Elliott SU(3) model [2]. The symplectic model with $\mathrm{Sp}(3,\mathbb{R})$-preserving interactions has achieved a remarkable reproduction of rotational bands and transition rates without the need for introducing effective charges, while only a single $\mathrm{Sp}(3,\mathbb{R})$ configuration is used [7, 9]. A shell-model study in a symplectic basis that allows for mixing of $\mathrm{Sp}(3,\mathbb{R})$ configurations due to pairing and non-degenerate single-particle energies above a ^{16}O core [8] has found that using only seven $\mathrm{Sp}(3,\mathbb{R})$ configurations is sufficient to achieve a remarkable reproduction of the ^{20}Ne energy spectrum as well as of $E2$ transition rates without effective charges.

3.1. The $\mathfrak{sp}(3,\mathbb{R})$ algebra and generators

As described in [38], the translationally invariant (intrinsic) symplectic generators can be written as SU(3) tensor operators in terms of the HO raising, $b^{\dagger(1\,0)}_{i\alpha} = \frac{1}{\sqrt{2}}(X_{i\alpha} - iP_{i\alpha})$, and lowering $b^{(0\,1)}_{i\alpha}$ dimensionless operators (with $\mathbf{X}$ and $\mathbf{P}$ the lab-frame position and momentum coordinates and $\alpha = 1, 2, 3$ for the three spatial directions) [7],

$$A^{(2\,0)}_{\mathfrak{L}M} = \frac{1}{\sqrt{2}}\sum_{i=1}^{A}\left[b^{\dagger}_{i}\times b^{\dagger}_{i}\right]^{(2\,0)}_{\mathfrak{L}M} - \frac{1}{\sqrt{2}A}\sum_{s,t=1}^{A}\left[b^{\dagger}_{s}\times b^{\dagger}_{t}\right]^{(2\,0)}_{\mathfrak{L}M} \tag{2}$$

$$C^{(1\,1)}_{\mathfrak{L}M} = \sqrt{2}\sum_{i=1}^{A}\left[b^{\dagger}_{i}\times b_{i}\right]^{(1\,1)}_{\mathfrak{L}M} - \frac{\sqrt{2}}{A}\sum_{s,t=1}^{A}\left[b^{\dagger}_{s}\times b_{t}\right]^{(1\,1)}_{\mathfrak{L}M}, \tag{3}$$

together with $B^{(0\,2)}_{\mathcal{L}M} = (-)^{\mathcal{L}-M}(A^{(2\,0)}_{\mathcal{L}-M})^{\dagger}$ ($\mathcal{L} = 0, 2$) and $H^{(00)}_{00} = \sqrt{3}\sum_i \left[b^{\dagger}_{i}\times b_{i}\right]^{(00)}_{00} - \frac{\sqrt{3}}{A}\sum_{s,t}\left[b^{\dagger}_{s}\times b_{t}\right]^{(00)}_{00} + \frac{3}{2}(A-1)$, where the sums run over all A particles of the system. The eight generators $C^{(1\,1)}_{\mathcal{L},M}$ ($\mathcal{L} = 1, 2$) close the $\mathfrak{su}(3)$ subalgebra of $\mathfrak{sp}(3,\mathbb{R})$. They realize the angular momentum operator:

$$L_{1M} = C^{(1\,1)}_{1M},\ M = 0, \pm 1, \tag{4}$$

and the Elliott algebraic quadrupole moment tensor $\mathcal{Q}^{a}_{2M} = \sqrt{3}C^{(1\,1)}_{2M}$, $M = 0, \pm 1, \pm 2$. The mass quadrupole moment can be constructed in terms of the symplectic generators as,

$$Q_{2M} = \sqrt{3}(A^{(2\,0)}_{2M} + C^{(1\,1)}_{2M} + B^{(0\,2)}_{2M}). \tag{5}$$

Equivalently, the symplectic generators, being one-body-plus-two-body operators can be expressed in terms of the creation operators $a^{\dagger}_{(\eta\,0)} = a^{\dagger}_{\eta}$, which create a nucleon in the HO shell $\eta = 0, 1, 2, \ldots$, together with its SU(3)-conjugate annihilation operator, $\tilde{a}_{(0\,\eta)}$. This is achieved by using the known matrix elements of the position ($\mathbf{X}_i$) and momentum ($\mathbf{P}_i$) operators in a HO basis, and hence, e.g., the first sum of $A^{(2\,0)}_{\mathfrak{L}M}$ in Eq. (2) becomes, $\sum_\eta \sqrt{\frac{(\eta+1)(\eta+2)(\eta+3)(\eta+4)}{12}}\left[a^{\dagger}_{(\eta+2\,0)}\times \tilde{a}_{(0\,\eta)}\right]^{(2\,0)}_{\mathfrak{L}M}$ [39]. Note that this operator describes excitations of a nucleon from the η shell to the $\eta+2$ shell, which corresponds to creating two single-particle HO excitation quanta, as manifested in the first term of Eq. (2).

Finally, the translationally invariant generators can be realized in terms of intrinsic coordinates, that is, particle position ($\mathbf{r}_i$) and momentum ($\mathbf{p}_i$) coordinates relative to the CM ($\sum_i \mathbf{r}_i = 0$ and $\sum_i \mathbf{p}_i = 0$), and, e.g., Eq. (2) becomes, $A^{(2\,0)}_{\mathfrak{L}M} = \frac{1}{\sqrt{2}}\sum_i \left[(b^{\dagger}_{i} - \frac{1}{A}\sum_s b^{\dagger}_{s})\times(b^{\dagger}_{i} - \frac{1}{A}\sum_t b^{\dagger}_{t})\right]^{(2\,0)}_{\mathfrak{L}M} \equiv \frac{1}{\sqrt{2}}\sum_{i=1}^{A}\left[\mathfrak{b}^{\dagger}_{i}\times\mathfrak{b}^{\dagger}_{i}\right]^{(2\,0)}_{\mathfrak{L}M}$, with the dimensionless intrinsic operators, $\mathfrak{b}^{\dagger(1\,0)}_{i\alpha} = \frac{1}{\sqrt{2}}(r_{i\alpha} - ip_{i\alpha})$.

3.2. Irreducible representations and many-body basis states

A many-body basis state of a symplectic irrep (detailed in [7]) is labeled according to the group chain,

$$\begin{array}{ccccccccc} \mathrm{Sp}(3,\mathbb{R}) & \supset & U(3) & \supset & \mathrm{SO}(3) & \supset & SO(2) \\ \sigma & & n\rho & \omega & \kappa & L & & M \end{array} \tag{6}$$

and constructed by acting with symmetrically coupled polynomials in the symplectic raising operators, $A^{(2\,0)}$, on a unique symplectic bandhead configuration, $|\sigma\rangle$,

$$|\sigma n\rho\omega\kappa LM\rangle = \left[\left[A^{(2\,0)}\times A^{(2\,0)}\ldots\times A^{(2\,0)}\right]^{n}\times|\sigma\rangle\right]^{\rho\omega}_{\kappa LM}, \tag{7}$$

where $\sigma \equiv N_\sigma\,(\lambda_\sigma\,\mu_\sigma)$ labels the $\mathrm{Sp}(3,\mathbb{R})$ irrep, $n \equiv N_n\,(\lambda_n\,\mu_n)$, $\omega \equiv N_\omega\,(\lambda_\omega\,\mu_\omega)$, and $N_\omega = N_\sigma + N_n$ is the total number of HO quanta (ρ and κ are multiplicity labels). This can be generalized to include spin, $|\sigma n\rho\omega\kappa(LS_\sigma)JM_J\rangle = \sum_{MM_S}\langle LM;S_\sigma M_S|\,JM_J\rangle|\sigma n\rho\omega\kappa LMS_\sigma M_S\rangle$, and also isospin. States within a symplectic irrep have the same spin (isospin) value, which is given by the spin S_σ (isospin T_σ) of the bandhead $|\sigma;S_\sigma(T_\sigma)\rangle$ [40]. Symplectic basis states span the entire shell-mode space. A complete set of labels includes additional quantum numbers $|\{\alpha\}\,\sigma\rangle$ that distinguish different bandheads with the same $N_\sigma\,(\lambda_\sigma\,\mu_\sigma)$. $\mathrm{Sp}(3,\mathbb{R})$-preserving Hamiltonians render energy spectra degenerate with respect to $\{\alpha\}$. However, for all present calculations for *gs* rotational bands and associated observables, $\{\alpha\}$ is unique (an only set).

The symplectic structure accommodates relevant particle-hole (p-h) configurations in a natural way (see also Fig. 1 of Ref. [12]). According to Eq. (7), the basis states of an $\mathrm{Sp}(3,\mathbb{R})$ irrep are built over a bandhead $|\sigma\rangle$ by $2\hbar\Omega$ 1p-1h (one particle raised by two shells) monopole ($\mathfrak{L}=0$) or quadrupole ($\mathfrak{L}=2$) excitations, realized by the first term in $A^{(2\,0)}_{\mathfrak{L}M}$ of Eq. (2), together with a smaller $2\hbar\Omega$ 2p-2h correction for eliminating the spurious center-of-mass motion, realized by the second term in $A^{(2\,0)}_{\mathfrak{L}M}$. The symplectic bandhead $|\sigma\rangle$ is the lowest-weight $\mathrm{Sp}(3,\mathbb{R})$ state, which is defined by the usual requirement that the symplectic lowering operators annihilate it. The bandhead, $|\sigma;\kappa_\sigma L_\sigma M_\sigma\rangle$, is an SU(3)-coupled many-body state with a given nucleon distribution over the HO shells and while not utilized here, can be obtained in terms of the above-mentioned creation operators $a^\dagger_{(\eta\,0)} = a^\dagger_\eta$. E.g., for a $0\hbar\Omega$ bandhead, the nucleon distribution is a single configuration,

$$\left[a^\dagger_{(\eta_1\,0)}\times a^\dagger_{(\eta_2\,0)}\times\ldots\times a^\dagger_{(\eta_A\,0)}\right]^{(\lambda_\sigma\,\mu_\sigma)}_{\kappa_\sigma L_\sigma M_\sigma}|0\rangle \tag{8}$$

with $N_\sigma = \eta_1+\eta_2+\ldots+\eta_A+\frac{3}{2}(A-1)$, such that $N_\sigma\hbar\Omega$ includes the HO zero-point energy. Note that 3/2 is subtracted from N_σ to ensure a proper treatment of the CM – in addition to this, the NCSpM uses translationally invariant symplectic generators that can be expressed in $\mathbf{r}_i$ and $\mathbf{p}_i$ relative to the CM; these symplectic generators are used to build the basis, the interaction, the many-particle kinetic energy operator, as well as to evaluate observables.

An example for the basis states within a symplectic irrep follows for ^{24}Mg. Its lowest HO-energy configuration is given by $N_\sigma = 62.5$ or $0\hbar\Omega$ (no HO excitation quanta), while the $4\hbar\Omega$ (20 0) symplectic irrep includes:

(i) A bandhead ($N_n = 0$) with $N_\sigma = 66.5$ (or $4\hbar\Omega$) and $(\lambda_\sigma\,\mu_\sigma) = (20\,0)$;

(ii) $N_n = 2$ states with N_ω=68.5 and $(\lambda_\omega\,\mu_\omega) = (22\,0)$, $(20\,1)$, and $(18\,2)$;

(iii) and so forth for higher N_n.

For each $(\lambda_\omega\,\mu_\omega)$, the quantum numbers κ, L and M are given by Elliott [2, 4]. E.g., for $(22\,0)$, $\kappa = 0$, $L = 0, 2, 4, \ldots, 22$, and $M = -L, -L+1, \ldots, L$.

3.3. Reduced matrix elements of the symplectic generators

The SU(3)-reduced matrix elements of the $\mathrm{Sp}(3,\mathbb{R})$ generators are analytically known [7,41–44]. The steps to compute $\langle \sigma n_f \rho_f \omega_f \| A^{(2\,0)} \| \sigma n_i \rho_i \omega_i \rangle$, similarly for $B^{(0\,2)}_{\mathcal{L}M} = (-)^{\mathcal{L}-M}(A^{(2\,0)}_{\mathcal{L}-M})^\dagger$, are outlined in what follows:

(i) Calculations of non-normalized matrix elements $(n_f \| \mathcal{A}^{(2\,0)} \| n_i)$ (with $A^{(2\,0)} \to \mathcal{A}^{(2\,0)}$ in the contraction u(3) [Weyl] limit) using Eq. (4.51) of Ref. [7] (see also, [41]) with $n_1 = \frac{N_n+2\lambda_n+\mu_n}{3}$, $n_2 = \frac{N_n-\lambda_n+\mu_n}{3}$, and $n_3 = \frac{N_n-\lambda_n-2\mu_n}{3}$ associated with $n_i = N_{n,i}\,(\lambda_{n,i}\,\mu_{n,i})$ and n_f (note that Ref. [7] uses '$a^\dagger$' instead of '$\mathcal{A}^{(2\,0)}$', not to be confused with the creation fermion operator referenced above);

(ii) Calculations of non-normalized $(\sigma n_f \rho_f \omega_f \| \mathcal{A}^{(2\,0)} \| \sigma n_i \rho_i \omega_i)$ from $(n_f \| \mathcal{A}^{(2\,0)} \| n_i)$ using Eq. (4.50) of Ref. [7];

(iii) Calculations of $\langle \sigma n_f \rho_f \omega_f \| A^{(2\,0)} \| \sigma n_i \rho_i \omega_i \rangle$ from the non-normalized reduced matrix elements (step 2) using the $\mathcal{K}$-matrix approach [42, 43]. The present calculations utilize the full $\mathcal{K}$ matrix (exact calculations). However, in the multiplicity-free case ($\rho_i^{\max} = \rho_f^{\max} = 1$) or in the limit of large σ [45], the normalization matrix reduces to normalization coefficients (a diagonal $\mathcal{K}$ matrix) given by Eq. (17) of Ref. [45].

For the $C^{(1\,1)}_{\mathfrak{L}M}$ SU(3)-reduced matrix elements, see, e.g., Eq. (19) of Ref. [44]. Using the reduced matrix elements of the $\mathrm{Sp}(3,\mathbb{R})$ generators and the relation (5), the analytical formula for the $Q \cdot Q$ matrix elements has been derived in Ref. [44].

For example, $\mathrm{Sp}(3,\mathbb{R})$-preserving Hamiltonians can include the many-particle kinetic energy:

$$\frac{T}{\hbar\Omega} = \frac{1}{\hbar\Omega}\sum_i \frac{\mathbf{p}_i^2}{2m} = \frac{1}{2}H^{(00)}_{00} - \sqrt{\frac{3}{8}}(A^{(2\,0)}_{00} + B^{(0\,2)}_{00}), \tag{9}$$

the HO potential:

$$\frac{V_{HO}}{\hbar\Omega} = \frac{1}{\hbar\Omega}\sum_i \frac{m\Omega^2\mathbf{r}_i^2}{2} = \frac{1}{2}H^{(00)}_{00} + \sqrt{\frac{3}{8}}(A^{(2\,0)}_{00} + B^{(0\,2)}_{00}), \tag{10}$$

as well as terms dependent on L, see Eq. (4), and Q, see Eq. (5). These interactions have analytical matrix elements in the symplectic basis (7) and act within a symplectic irrep ($\sigma_f = \sigma_i \equiv \sigma$). For example, for the dimensionless many-particle kinetic energy, $\frac{T}{\hbar\Omega}$, the matrix elements are given as:

$$\begin{aligned}
&\left\langle \sigma n_f \rho_f \omega_f \kappa_f L_f M_f | \frac{T}{\hbar\Omega} | \sigma n_i \rho_i \omega_i \kappa_i L_i M_i \right\rangle = \\
&\frac{1}{2}\left\langle \sigma n_f \rho_f \omega_f \kappa_f L_f M_f | H^{(00)}_{00} | \sigma n_i \rho_i \omega_i \kappa_i L_i M_i \right\rangle \\
&-\sqrt{\frac{3}{8}}\left\langle \sigma n_f \rho_f \omega_f \kappa_f L_f M_f | A^{(2\,0)}_{00} + B^{(0\,2)}_{00} | \sigma n_i \rho_i \omega_i \kappa_i L_i M_i \right\rangle = \\
&\frac{1}{2}N_\omega \delta_{f,i} - \sqrt{\frac{3}{8}}\left(\langle \omega_i \kappa_i L_i M_i; (2\,0)00 |\, \omega_f \kappa_f L_f M_f \rangle \langle \sigma n_f \rho_f \omega_f \| A^{(2\,0)} \| \sigma n_i \rho_i \omega_i \rangle + \text{conjugate} \right),
\end{aligned} \tag{11}$$

where $\langle \omega_i \kappa_i L_i M_i; (2\,0)00 |\, \omega_f \kappa_f L_f M_f \rangle$ is the SU(3) Clebsch-Gordan coefficient and the reduced matrix elements of the symplectic generators are calculated according to the steps outlined above.

4. Utilizing approximate symmetries in nuclear modeling

We employ the no-core symplectic model (NCSpM), outlined in Ref. [9], with a novel interaction that is effectively realized by an exponential dependence on the quadrupole-quadrupole ($Q.Q$) two-body interaction [12,38]. This introduces simple but important many-body interactions that enter in a prescribed hierarchical way given in powers of a small parameter, the only adjustable parameter in the model. The model offers a microscopic no-core shell-model description of nuclei in terms of mixed deformed configurations and allows the inclusion of higher-energy particle excitations [12] that are currently inaccessible by *ab initio* shell models. It reduces to the successful Elliott model [2,4] in the limit of a single valence shell and a zero model parameter.

The underlying groups of the NCSpM are the symplectic $\mathrm{Sp}(3,\mathbb{R})$ group [6,7] and its SU(3) subgroup [2,4]. The symplectic basis, described above and utilized in NCSpM, is related, via a unitary transformation (see the review [40]), to the three-dimensional HO (m-scheme) many-body basis used in the NCSM [13]. Indeed, the NCSpM employed within a complete model space up through $N_{\max}$, will coincide with the NCSM for the same $N_{\max}$ cutoff. Important features of the NCSpM model are (1) the $\mathrm{Sp}(3,\mathbb{R})$ irreps divide the space into 'vertical cones' that are comprised of basis states of good $(\lambda\,\mu)$ quantum numbers, and (2) its ability to down-select to the most relevant configurations, which are chosen among all possible $\mathrm{Sp}(3,\mathbb{R})$ irreps within an $N_{\max}$ model space.

4.1. Schematic many-nucleon interaction

As discussed in Ref. [12], we employ a microscopic many-body interaction, which allows for large $N_{\max}$ no-core shell-model applications. This interaction utilizes two central components: a single-particle piece, consisting of the harmonic oscillator potential and a spin-orbit term, together with a collective piece, which enters through the use of the quadrupole-quadrupole interaction. Specifically, we utilize an elementary form tied to a long-range expansion of the nucleon-nucleon central force $V(|\mathbf{r}_i-\mathbf{r}_j|)$ [46], simplified by considering the most relevant degrees of freedom necessary to describe deformed spatial configurations,

$$\begin{aligned} H_\gamma &= \sum_{i=1}^{A}\left(\frac{\mathbf{p}_i^2}{2m}+\frac{m\Omega^2\mathbf{r}_i^2}{2}-\kappa l_i\cdot s_i\right) \\ &\quad +\frac{\chi}{2}\frac{(e^{-\gamma(Q\cdot Q-\langle Q\cdot Q\rangle_{N_n})}-1)}{\gamma}, \end{aligned} \tag{12}$$

where $\hbar\Omega$, κ, and χ are parameters, for which we use empirical estimates, while $\gamma \geq 0$ is the only adjustable parameter in the model (as discussed below). H_γ is given in terms of particle momentum and position coordinates relative to the center of mass. The average contribution $\langle Q\cdot Q\rangle_{N_n}$ of $Q\cdot Q$ for given N_n HO excitations [47] introduces a considerable renormalization of the HO shell structure and hence, is removed in multi-shell studies [35].

We use $\chi = \hbar\Omega/(4\sqrt{N_{\omega(f)}N_{\omega(i)}})$ for a $\langle f|H_\gamma|i\rangle$ matrix element for final (f) and initial (i) many-body states. The decrease of χ with N_ω, to leading order in λ/N_ω, has been shown by Rowe [48] based on self-consistent arguments. We also use the empirical estimates $\hbar\Omega \approx 41/A^{1/3} = 18$ MeV and $\kappa \approx 20/A^{2/3} = 3.8$ MeV (e.g., see [1]). The only adjustable parameter of the NCSpM model is γ, which controls the presence of the many-body interactions and thus cannot be informed by existing two-body and three-body interactions. The effective interaction (12) introduces hierarchical many-body interactions in a prescribed way, e.g.,

$$\frac{\chi}{2\gamma}\left(e^{-\gamma Q\cdot Q}-1\right) = -\frac{1}{2}[\chi(\sum_{k=0}^{\infty}\frac{(-\gamma)^k(Q\cdot Q)^k}{(k+1)!})]Q\cdot Q, \tag{13}$$

such that they become quickly negligible for a reasonably small $\gamma \ll 1$. E.g., we find that for ^{12}C, besides $Q\cdot Q$, only one term is sufficient for the ground-state band ($k=1$), while three

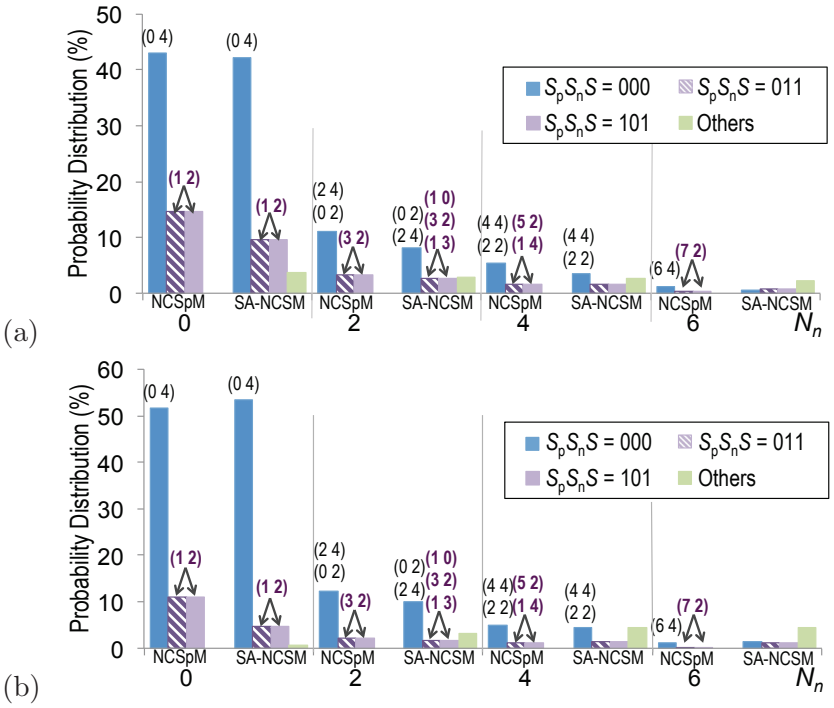

Figure 2. Probability distribution for ^{12}C as a function of the N_n total excitations of (a) the lowest 0^+ state and (b) the lowest 4^+ state as calculated by the NCSpM with H_γ (left set of bars within each N_n value) and the *ab initio* SA-NCSM with the bare JISP16 NN interaction (right set of bars within each N_n value). Both models are limited to an $N_{\max} = 6$ model space for comparison. The dominant shape deformations, specified by $(\lambda\,\mu)$, are shown. Very similar results are obtained for the lowest 2^+ state.

terms ($k = 3$) are sufficient for the Hoyle-state band [12]. This ties directly to the interaction used in Ref. [49], which is given as a polynomial in Q, namely, $Q \cdot Q$, $(Q \times Q) \cdot Q$, and $(Q \cdot Q)^2$, and applied to the ^{24}Mg *gs* rotational band.

4.2. Comparison to ab initio *no-core shell model*

A comparison of the present NCSpM results for ^{12}C to *ab initio* outcomes is possible in smaller model spaces, for example, for the *gs* rotational band in $N_{\max} = 6$. This space appears to be reasonable for these states for both models. In particular, we compare to wavefunctions obtained in the SA-NCSM [50] with the bare JISP16 realistic interaction [37]. Consistent with the outcome of Refs. [50] and [11] (see, e.g., Fig. 1 in Ref. [11] for ^{6}Li and ^{8}Be wavefunctions in $N_{\max} = 8 - 10$, as well as Fig. 1 above), the *ab initio* $N_{\max} = 6$ SA-NCSM results for the 0^+ *gs*, first 2^+ and first 4^+ states of ^{12}C reveal the dominance of the $0\hbar\Omega$ component with the foremost contribution coming from the leading $(0\,4)$ $S = 0$ irrep (see Fig. 2 for the *gs* and the 4^+_1 state). Furthermore, we find that important SU(3) configurations are then organized into structures according to the Sp$(3,\mathbb{R})$ symplectic group, that is, the $(0\,4)$ symplectic irrep gives rise to dominant $(0\,2)$ and $(2\,4)$ configurations in the $2\hbar\Omega$ subspace and so on (see Fig. 2), similarly to the discussion above for the ^{8}Be ground state. The next important configuration is spin-1 $(1\,2)$ at $0\hbar\Omega$ with the associated symplectic excitations (Fig. 2). Therefore, among all possible configurations present in the SA-NCSM, only the states of the $(0\,4)$ and then $(1\,2)$ symplectic irreps appear dominant.

In addition, we find a close similarity to *ab initio* results for the NCSpM wavefunctions of

the *gs* rotational band, calculated with H_γ (12) for $\gamma = 0.74 \times 10^{-4}$ and symplectic irreps with bandheads (0 4) and (1 2) (Fig. 2). NCSpM and SA-NCSM calculations are performed for $\hbar\Omega = 18$ and $N_{\max} = 6$ model spaces. The close agreement of the probability distribution across the $N_n\hbar\Omega$ subspaces and of the SU(3) content of the wavefunctions for the two models indicates that the two $0\hbar\Omega$ bandheads of the NCSpM model space account for the part of the complete $N_{\max} = 6$ model space that is most relevant to the physics of the ^{12}C *gs* rotational band. If the SA-NCSM model space is reduced to only the spin components used in this study, $S_pS_nS = 000$, 011, and 101, NCSpM observables such as *gs* matter rms radius and $Q_{2_1^+}$ reproduce their *ab initio* counterparts as much as 80-90% and 70-90%, respectively, for the same $\hbar\Omega$ and $N_{\max} = 2$, 4 and 6. This suggests that the interaction used in NCSpM has effectively captured a major portion of the underlying physics of the realistic interaction important to the low-lying nuclear states [12].

4.3. Clustering and collectivity in ^{12}C

The NCSpM outcome reveals a quite remarkable agreement with the experiment (Fig. 3a). The results are shown for $N_{\max} = 20$, which we found sufficient to yield convergence. This $N_{\max}$ model space is further reduced by selecting the most relevant symplectic irreps, namely, five symplectic bandheads and all symplectic multiples thereof up through $N_{\max} = 20$ of total dimensionality of 6.6×10^3. The four bandheads are the spin-zero ($S = 0$) $0\hbar\Omega$ 0p-0h (0 4), $2\hbar\Omega$ 2p-2h (6 2), and $4\hbar\Omega$ 4p-4h (12 0) symplectic bandheads together with the $S = 1$ $0\hbar\Omega$ 0p-0h (1 2). In comparison to experiment, the outcome (Fig. 3a, dark colors) reveals that the lowest 0^+, 2^+, and 4^+ states of the 0p-0h symplectic irreps (Fig. 3a, blue) calculated with $\gamma = -1.71 \times 10^{-4}$ closely reproduce the *gs* rotational band, indicating clear oblate shapes (Fig. 3b, top). In addition, the calculated lowest states of the $4\hbar\Omega$ 4p-4h (12 0) irrep (Fig. 3a, red) are found to lie close to the Hoyle-state rotational band, revealing alpha-clustering and prolate shapes (Fig. 3b, bottom). Furthermore, the lowest 0^+ of the $2\hbar\Omega$ 2p-2h (6 2) irrep (Fig. 3a, green) is found to lie around the 10-MeV 0^+ resonance (third 0^+ state).

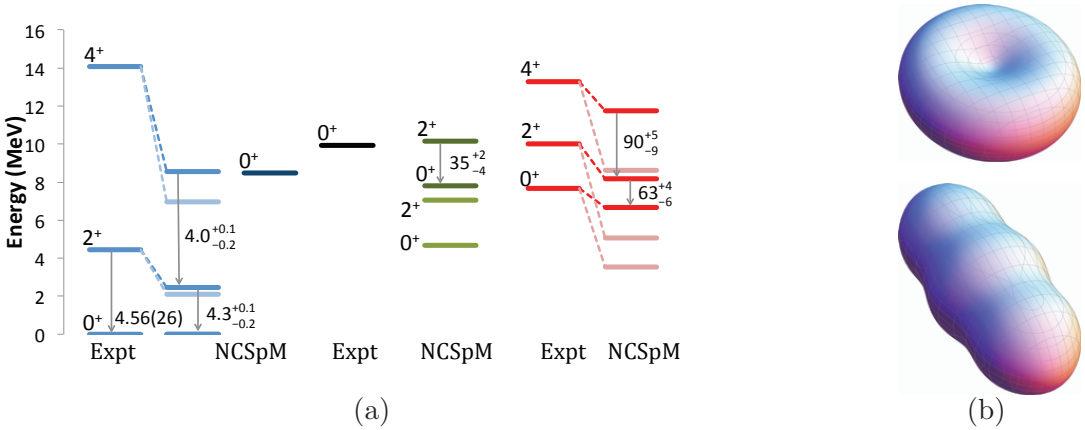

Figure 3. (a) Energy spectrum for ^{12}C calculated using NCSpM in the $N_{\max} = 20$ model space of $Sp(3,\mathbb{R})$ irreps with $N_\sigma = 24.5$ (blue, left), $N_\sigma = 26.5$ (green, middle), and $N_\sigma = 28.5$ (red, right), and $(\lambda_\sigma\, \mu_\sigma) = (0\,4)$, (6 2), and (12 0) (light colors) and with the addition of the (1 2) $Sp(3,\mathbb{R})$ irrep (dark colors). Experimental data is from [51], except the latest results for 0_3^+ [28] and the states above the Hoyle state, 2^+ [31] and 4^+ [52]. $B(E2)$ transition rates are in W.u. with theoretical uncertainties estimated for a ±60% deviation of the Hoyle state energy. (b) NCSpM matter-density profile (with respect to the intrinsic frame) of the ^{12}C ground state (top) and the Hoyle state (bottom) showing the formation of three clusters in the Hoyle state within a no-core shell-model framework.

As compared to the model space consisting of the spin-0 irreps only (Fig. 3a, light colors), the addition of only one spin-1 irrep yields a NCSpM energy spectrum that is further improved and found to lie reasonably close to the experimental data. The $\mathrm{Sp}(3,\mathbb{R})$-nonpreserving spin-orbit term mixes the spin-0 $(0\,4)$ and spin-1 $(1\,2)$ irreps for all $J^\pi = 0^+$, 2^+_1, and 4^+_1, which results in a more realistic energy spacing between the excited states. Specifically, we see the *gs* separating from the higher-lying 0^+ states, and a slight stretching in the *gs* rotational band. This is similar to the findings of early cluster models, which remedy this by allowing for alpha-cluster dissociation due to a spin-orbit force as discussed in [24].

The outcome of the present analysis is not limited to ^{12}C. The model we find is also applicable to the low-lying states of other *p*-shell nuclei, such as ^{8}Be, as well as *sd*-shell nuclei without any adjustable parameters [38, 53]. In particular, using the same $\gamma = -1.71 \times 10^{-4}$ as determined for ^{12}C, we describe selected low-lying states in ^{8}Be in an $N_{\max} = 24$ model space with only 3 spin-zero $0\hbar\Omega$ $(4\,0)$, $2\hbar\Omega$ $(6\,0)$, and $4\hbar\Omega$ $(8\,0)$ symplectic irreps [53]. Furthermore, we have successfully applied the NCSpM without any adjustable parameters to the *gs* rotational band of heavier nuclei, such as ^{20}O, ^{20,22,24}Ne, ^{20,22}Mg, and ^{24}Si [38]. This suggests that the fully microscopic NCSpM model has indeed captured an important part of the physics that governs the low-energy nuclear dynamics and informs key features of the interaction and nuclear structure primarily responsible for the formation of such simple patterns.

In short, by utilizing approximate symmetries that are found to underpin nuclear dynamics, we offer a novel framework, based on the no-core shell model, to further understand highly deformed states, exemplified by the Hoyle state and its rotational band.

Acknowledgments

We thank D. Rowe and G. Rosensteel, as well as the PetaApps Collaboration, in particular, J. P. Vary and P. Maris, for useful discussions. This work was supported by the U.S. NSF (OCI-0904874), the U.S. DOE (DE-SC0005248), and SURA. ACD acknowledges support by the U.S. NSF (grant 1004822) through the REU Site in Dept. of Physics & Astronomy at LSU. We also acknowledge DOE/NERSC, LSU/LONI, and NSF & U. of Illinois/Blue Waters for providing HPC resources.

References

[1] Bohr A and Mottelson B R 1969 *Nuclear Structure* vol 1 (New York: Benjamin)
[2] Elliott J P 1958 *Proc. Roy. Soc. A* **245** 128
[3] Elliott J P 1958 *Proc. Roy. Soc. A* **245** 562
[4] Elliott J P and Harvey M 1962 *Proc. Roy. Soc. A* **272** 557
[5] Hecht K T 1971 *Nucl. Phys. A* **170** 34
[6] Rosensteel G and Rowe D J 1977 *Phys. Rev. Lett.* **38** 10
[7] Rowe D J 1985 *Reports on Progr. in Phys.* **48** 1419
[8] Draayer J, Weeks K and Rosensteel G 1984 *Nucl. Phys.* **A419** 1
[9] Bahri C and Rowe D J 2000 *Nucl. Phys. A* **662** 125
[10] Vargas C, Hirsch J and Draayer J 2001 *Nucl. Phys. A* **690** 409
[11] Dytrych T, Launey K D, Draayer J P, Maris P, Vary J P, Saule E, Catalyurek U, Sosonkina M, Langr D and Caprio M A 2013 *Phys. Rev. Lett.* **111** 252501
[12] Dreyfuss A C, Launey K D, Dytrych T, Draayer J P and Bahri C 2013 *Phys. Lett. B* **727** 511
[13] Navrátil P, Vary J P and Barrett B R 2000 *Phys. Rev. Lett.* **84** 5728
[14] Maris P, Shirokov A M and Vary J P 2010 *Phys. Rev. C* **81** 021301(R)
[15] Navrátil P, Quaglioni S, Stetcu I and Barrett B R 2009 *J. Phys. G: Nucl. Part.* **36** 083101
[16] Roth R and Navrátil P 2007 *Phys. Rev. Lett.* **99** 092501
[17] Abe T, Maris P, Otsuka T, Shimizu N, Utsuno Y and Vary J 2012 *Phys. Rev. C* **86** 054301
[18] Pieper S C, Varga K and Wiringa R B 2002 *Phys. Rev. C* **66** 044310
[19] Wloch M, Dean D J, Gour J R, Hjorth-Jensen M, Kowalski K, Papenbrock T and Piecuch P 2005 *Phys. Rev. Lett.* **94** 212501

[20] Tsukiyama K, Bogner S K and Schwenk A 2011 *Phys. Rev. Lett.* **106** 222502
[21] Epelbaum E, Krebs H, Lee D and Meissner U G 2011 *Phys. Rev. Lett.* **106** 192501
[22] Hoyle F 1954 *Astrophys. J. Suppl. Ser.* **1** 121
[23] Chernykh M, Feldmeier H, Neff T, von Neumann-Cosel P and Richter A 2007 *Phys. Rev. Lett.* **98** 032501
[24] Khoa D T, Cuonga D C and Kanada-En'yo Y 2011 *Phys. Letts. B* **695** 469
[25] Fynbo H O U *et al.* 2005 *Nature* **433** 136
[26] Freer M *et al.* 2009 *Phys. Rev. C* **80** 041303
[27] Hyldegaard S *et al.* 2010 *Phys. Rev. C* **81** 024303
[28] Itoh M *et al.* 2011 *Phys. Rev. C* **84** 054308
[29] Zimmerman W R, Destefano N E, Freer M, Gai M and Smit F D 2011 *Phys. Rev. C* **84** 027304
[30] Raduta A R *et al.* 2011 *Phys. Letts. B* **705** 65
[31] Zimmerman W R *et al.* 2013 *Phys. Rev. Lett.* **110** 152502
[32] Marin-Lambarri D J, Bijker R, Freer M, Gai M, Kokalova T, Parker D and Wheldon C 2014 *Phys. Rev. Lett.* **113** 012502
[33] Rosensteel G and Rowe D J 1977 *Ann. Phys. N.Y.* **104** 134
[34] Leschber Y and Draayer J P 1987 *Phys. Letts. B* **190** 1
[35] Castaños O, Draayer J P and Leschber Y 1988 *Z. Phys. A* **329** 33
[36] Entem D R and Machleidt R 2003 *Phys. Rev. C* **68** 041001
[37] Shirokov A, Vary J, Mazur A and Weber T 2007 *Phys. Lett. B* **644** 33
[38] Tobin G K, Ferriss M C, Launey K D, Dytrych T, Draayer J P and Bahri C 2014 *Phys. Rev. C* **89** 034312
[39] Escher J and Draayer J P 1999 *Phys. Rev. Lett.* **82** 5221
[40] Dytrych T, Sviratcheva K D, Draayer J P, Bahri C and Vary J P 2008 *J. Phys. G: Nucl. Part. Phys.* **35** 123101
[41] Rosensteel G and Rowe D J 1983 *J. Math. Phys.* **24** 2461
[42] Rowe D 1984 *J. Math. Phys.* **25** 2662
[43] Hecht K 1985 *J. Phys. A* **18** L1003
[44] Rosensteel G 1990 *Phys. Rev. C* **42** 2463
[45] Rowe D, Rosensteel G and Carr R 1984 *J. Phys. A: Math. Gen.* **17** L399
[46] Harvey M 1968 *Adv. Nucl. Phys.* **1** 67
[47] Rosensteel G and Draayer J P 1985 *Nucl. Phys. A* **436** 445
[48] Rowe D J 1967 *Phys. Rev.* **162** 866
[49] Peterson D and Hecht K 1980 *Nucl. Phys. A* **344** 361
[50] Dytrych T, Maris P, Launey K D, Draayer J P, Vary J P, Caprio M, Langr D, Catalyurek U and Sosonkina M 2014 *to be submitted to Phys. Rev. C*
[51] Ajzenberg-Selove F and Kelley J 1990 *Nucl. Phys. A* **506** 1
[52] Freer M *et al.* 2011 *Phys. Rev. C* **83** 034314
[53] Launey K D, Dytrych T, Draayer J P, Tobin G K, Ferriss M C, Langr D, Dreyfuss A C, Maris P, Vary J P and Bahri C 2013 Symmetry-adapted No-core Shell Model for Light Nuclei *Proceedings of the 5th International Conference on Fission and properties of neutron-rich nuclei, ICFN5, November 4 - 10, 2012, Sanibel Island, Florida, edited by J. H. Hamilton and A. V. Ramayya* (Singapore: World Scientific) p 29